



Dynamical properties and performances of β -Ga₂O₃ UVC photodetectors of extreme solar blindness

Luc Damé, Lucile Conan, Carlo de Santi, Alessandro Caria, Matteo Buffolo, Matteo Meneghini, Pierre Maso, Clément Dias, Halima Ghorbel, Pierre Gilbert, et al.

► To cite this version:

Luc Damé, Lucile Conan, Carlo de Santi, Alessandro Caria, Matteo Buffolo, et al.. Dynamical properties and performances of β -Ga₂O₃ UVC photodetectors of extreme solar blindness. Oxide-based Materials and Devices XIV. Proceedings Volume 12422, SPIE, Jan 2023, San Francisco, United States. pp.1242207, 10.1117/12.2651204 . insu-04040169

HAL Id: insu-04040169

<https://insu.hal.science/insu-04040169>

Submitted on 28 Nov 2023

HAL is a multi-disciplinary open access archive for the deposit and dissemination of scientific research documents, whether they are published or not. The documents may come from teaching and research institutions in France or abroad, or from public or private research centers.

L'archive ouverte pluridisciplinaire **HAL**, est destinée au dépôt et à la diffusion de documents scientifiques de niveau recherche, publiés ou non, émanant des établissements d'enseignement et de recherche français ou étrangers, des laboratoires publics ou privés.

Dynamical properties and performances of β -Ga₂O₃ UVC photodetectors of extreme solar blindness

Luc Damé^{*a}, Lucile Conan^a, Carlo De Santi^b, Alessandro Caria^b, Matteo Buffolo^b, Matteo Meneghini^b, Pierre Maso^c, Clément Dias^a, Halima Ghorbel^a, Pierre Gilbert^a, Mustapha Meftah^a, Philippe Bove^d, V. Sandana^d, David Rogers^d, Ferechteh Teherani^d

^aLATMOS, IPSL, CNRS, University Versailles Saint-Quentin en Yvelines, University Paris-Saclay, 11 boulevard d'Alembert, 78280 Guyancourt, France; ^bDipartimento di Ingegneria dell'Informazione, via Gradenigo 6/b, 35131 Padova, Italy; ^cPIT, OVSQ, 11 boulevard d'Alembert, 78280 Guyancourt, France; ^dNanovation, 8 route de Chevreuse, 78117 Châteaufort, France

*E-mail: luc.dame@latmos.ipsl.fr

ABSTRACT

There is a surge in interest for the ultra wide bandgap ($E_g \sim 4.9$ eV) semiconductor gallium oxide (Ga₂O₃). A key driver for this boom is that single crystal wide area bulk β -Ga₂O₃ substrates have become commercially available and that a variety of methods have been shown to give high quality epitaxial growth. Amongst a whole range of potential applications (power/switching electronics, solar transparent electrodes, etc.) extreme solar blindness photodetectors in β -Ga₂O₃, the more stable monoclinic phase of Ga₂O₃, offers the most exciting perspectives for deep ultraviolet observations below 250 nm. We present an overview of the complete realization process (epitaxy, photolithography, singulation and packaging), and space qualification (to TRL8) of a series of β -Ga₂O₃ photodetectors. We insist on their remarkable solar blindness performance (factor 1000 or more between peak responsivity around 215-220 nm and 250 nm) and dynamical properties (rise and fall times < 5 ms), along with their enhanced responsivity, excellent thermal behaviour and radiation hard properties. 4 of these detectors have been integrated on the INSPIRE-SAT 7 nanosatellite expected to be launched in April 2023 to reach the TRL9 "demonstrated in flight" qualification.

Keywords: Deep ultraviolet photodetectors, β -Ga₂O₃ oxide, Space observations, Dynamical properties, Herzberg continuum, Nanosatellites.

1. INTRODUCTION

We present the development of disruptive ultra wide band gap semiconductor (≥ 4.9 eV, corresponding to a 253 nm vacuum wavelength) UVC photodetectors on oxide-based β -Ga₂O₃ that are intrinsically solar blind, radiation-hard and thermally-robust. We have recently shown that the bandgap of these detectors can be engineered upwards through Al alloying, β -(Al)Ga₂O₃, so as to obtain optical transitions from 253 down to 200 nm [1]. The detectors developed and space qualified are intended to monitor the Solar Spectral Irradiance (SSI) at 215/220 nm (Herzberg solar continuum: 200–242 nm) with an accuracy better than 0.5% (5 times better than previous measurements in Space [2]).

In this paper we recall the realization process, properties and performance of these detectors and, in particular, the new evaluation of the dynamical response of these detectors (< 5 ms) largely under evaluated in a previous work [3] and even recently by a factor 2 [4]. 4 of these new β -Ga₂O₃-based photodetectors have been space qualified and integrated in the INSPIRE-7 nanosatellite [5] to be launched in April 2023. Already at TRL8 (qualified for flight) these detectors could reach the TRL9 level (demonstrated in flight) and, since of their very simple implementation process, they could be integrated in several of the Earth and climate constellations currently developed or planned to observe the UVC spectral band 200–242 nm of particular interest for climate (this solar spectral band, absorbed in the stratosphere, causes oxygen to dissociate and creates the ozone layer).

2. DETECTORS REALIZATION

We realized, from epitaxy to packaging (cf. Fig. 1), detectors in $\beta\text{-Ga}_2\text{O}_3$ sensitive between 200 and 240 nm, centred at 215-220 nm, with a half width at half maximum reduced (of the order of 30 nm) and with excellent rejection of the visible spectrum (a factor 1000 between the peak response at 215/220 nm and 250 nm). Oxide materials have this decisive advantage: a significant rejection of the visible adjustable in wavelength as a function of the oxide chosen and its doping (aluminium in our case [1]). $\beta\text{-(Al)Ga}_2\text{O}_3$ "solar blind" detectors also present an excellent signal-to-noise ratio (dark current is very low: ≤ 5 pA). These detectors have also other significant properties: they are radiation hard (long term performances) and performing at ambient temperature (no need for cooling).

These detectors were realized in the framework of the ANR DEVINS program (2018-2022) from the wafers to the final packaged sensors going through device architecture development, epitaxy, photolithography, contacting, probing, singulation and packaging in TO-39 caps with sapphire windows. Process is detailed in previous papers [1, 3, 4].

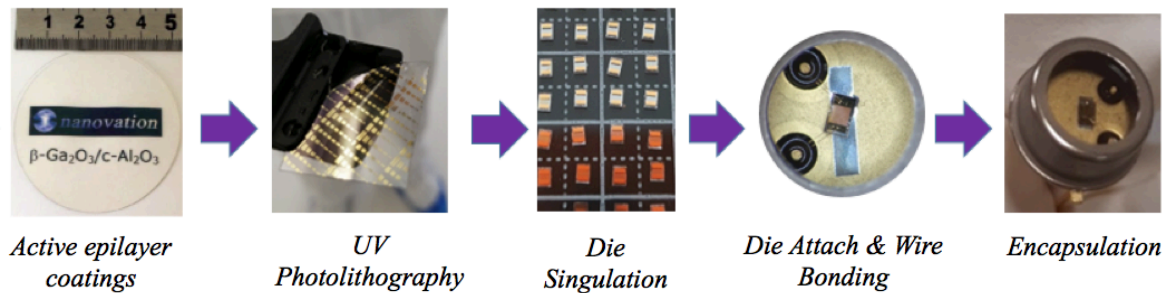


Figure 1. The 5 main steps in the device architecture development of the DEVINS UVC $\beta\text{-Ga}_2\text{O}_3$ detectors (epitaxy, photolithography, contacting, probing, singulation and packaging in TO-39 caps).

3. PERFORMANCE EVALUATION

We performed probing tests on hundreds of MSM components (5000 realized) to categorize detectors performances and to select a hundred of them for packaging and space qualification. So far, we achieved up to 6 orders of magnitude between dark and light currents at only -5 V bias voltage (constraint of nanosatellite finally released to -10 V). Dark current is very low (≤ 5 pA) and could not be measured most of the time with our equipment on the good selected components. Dynamics on its side (rise and fall times) has been thoroughly studied and better than expected with this material (less than 5 ms), and much better than reported, erroneously, to a few seconds in a previous work [3].

3.1 Dark current

The dark current was measured on hundreds of $\beta\text{-Ga}_2\text{O}_3$ Metal-Semiconductor-Metal (MSM) photodetectors and on the packaged detectors. Fig. 2 presents one of the result of its measurement on a packaged detector not selected for flight (low responsivity of 1 mA/W only). We notice an excellent 6 order of magnitude between dark and light currents measured at only -5 V bias voltage. Dark current, in addition, was very low ($< 5 \pm 1$ pA) and below the measurements capabilities of our equipment. 5 to 6 orders of magnitude were typically observed on packaged detectors when connectors are properly fixed (wire bonding) on an extra pad to strengthen the soldering process (see Fig. 4 in reference [4]). On the MSM, with probe contacts, only 3 to 4 orders of magnitude between dark and light are commonly observed [1] because of the poor contacts of limited size.

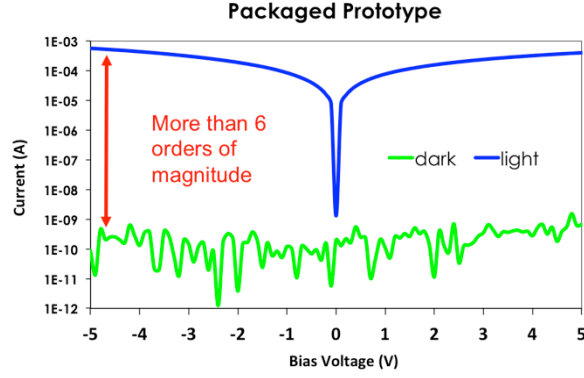


Figure 2. We observed 6 order of magnitude between dark and light currents measured at only -5 V bias voltage. Dark current is very low ($< 5 \pm 1$ pA) and below the measurements capabilities of our equipment.

3.2 Spectral response

A test bench set-up was developed at LATMOS to characterize the detectors using a Deuterium lamp and powermeter (cf. Fig. 3). Acquisition is automatized under computer control with a LabVIEW program.

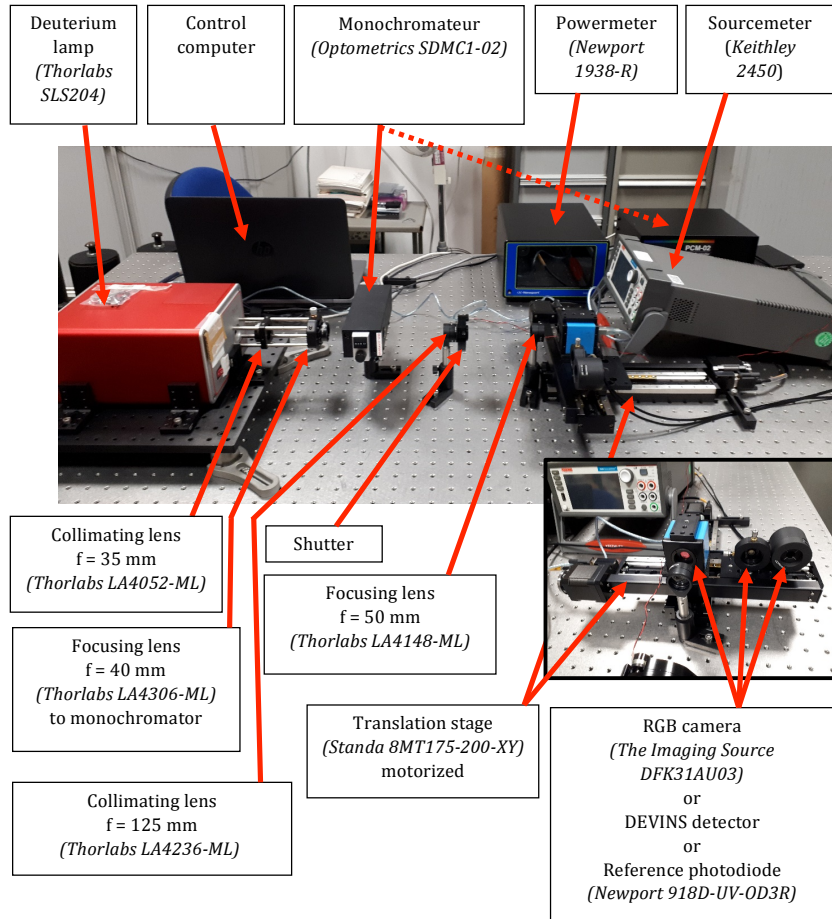


Figure 3. Characterization test bench developed at LATMOS for the photodetectors DEVINS in β -(Al)Ga₂O₃.

Fig. 4 shows a typical spectral response of our Gallium oxide detectors. They reveal a peak response of 10 to 70 mA/W at 215 nm and a FWHM of ~ 35 nm, compatible with our spectral range of interest between 200 and 242 nm.

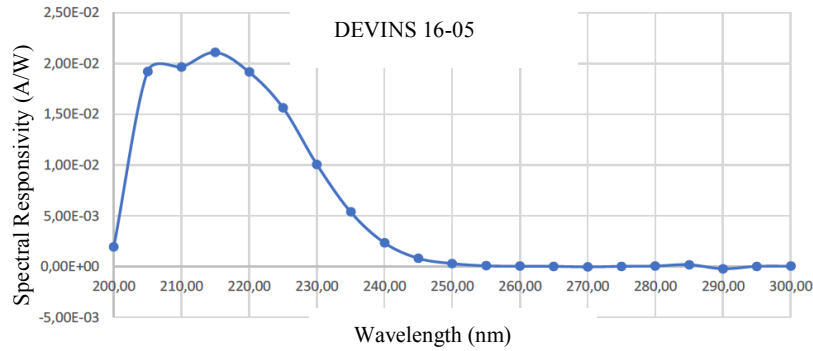


Figure 4. Typical spectral responsivity (in A/W) of a photodetector (707-26/16-05, selected for flight on INSPIRE-SAT 7) with a maximum at 215 nm, a response of ~ 20 mA/W (with a bias voltage of -5 V), an FWHM of ~ 35 nm and, accordingly, an excellent rejection of about 1000 for wavelengths above 250 nm.

Note that when the voltage is increased, e.g. to a bias voltage of 10 V instead of 5 V (a possibility implemented on the nanosatellite INSPIRE-SAT 7), the response is multiplied by a factor 5 to 7 owing the non-linearity of the response between 5 and 10 V (cf. Fig. 5). For example, measured packaged detectors 707-23 raised from 20 mA/W to 120 mA/W and 707-04 from 20 to 100 mA/W at peak value 220 nm.

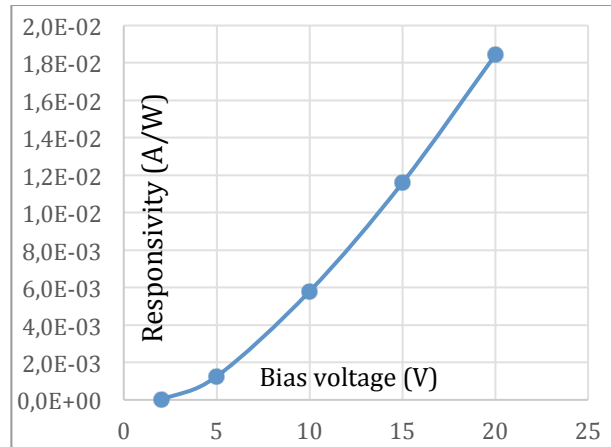


Figure 5. The spectral response of the photodetectors increases significantly as a function of the bias voltage. Between 5 and 10 V of bias voltage the multiplying factor on the responsivity is 5 to 7 while it is more linear after (factor 2 between 10 and 15 V; factor 3 between 10 and 20 V).

3.3 Dynamical response

Dynamical response (rise and fall times) were evaluated recently [4] to be less than 20 ms. In fact, and even if further work is still necessary, we established after correcting the power line noise (50 Hz) with a Notch filter (40-60 Hz), that this figure is even better: we were able to achieve reliable operation at 480 Hz and measured a stable response time (rise and fall times) of less than 5 ms (cf. Fig. 6).

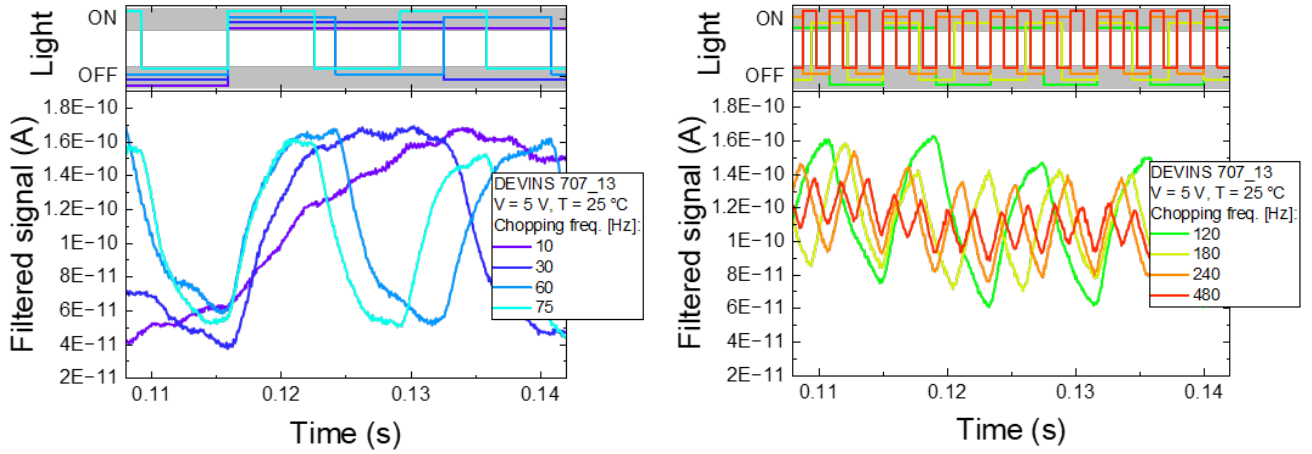


Figure 6. Steady-state time dependence of the photoresponse of a photodetector at 215 nm (bias of -5 V applied at start).

As soon as bias is applied to the photodetector, the photoresponse was found to start decreasing until a steady-state condition is reached (see Fig. 7). In order to have stable operation of the photodetector during the mission, the bias will be permanently applied when in use in space to avoid the decrease observed at start.

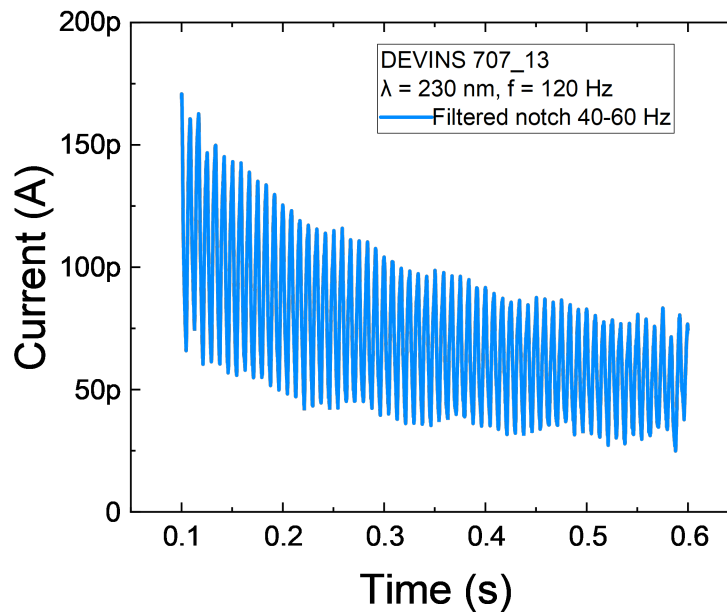


Figure 7. Time dependence of the photoresponse after bias is applied.

In order to investigate the physical process limiting the dynamic performance, the measurements were repeated at different ambient temperatures. As reported in Fig. 8, temperature has a significant impact on the speed and amplitude of the response. This behaviour can be caused by various effects, including the variation in leakage level with temperature and the change in defect capture and emission rate. A full analysis is not trivial and will be carried out in the future.

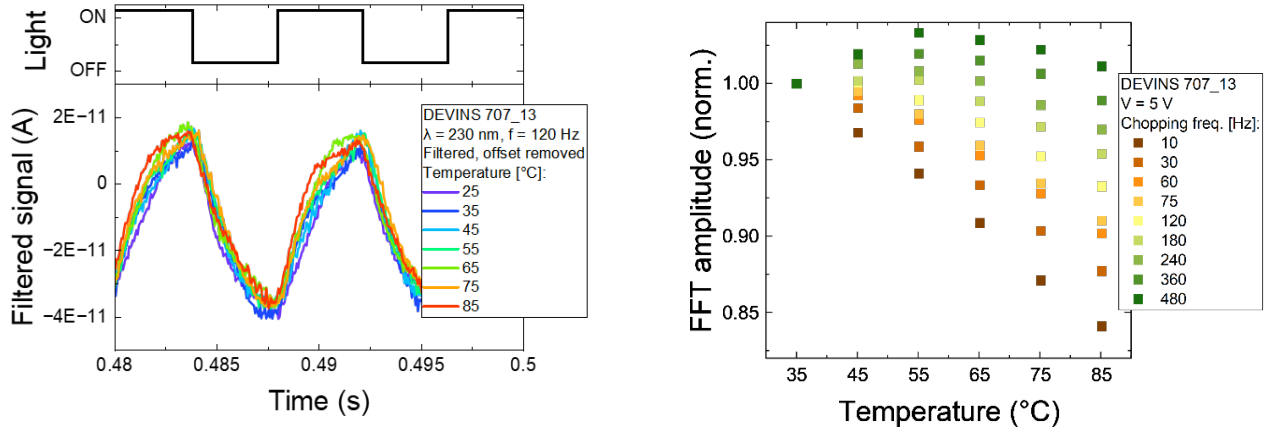


Figure 8. Temperature dependence of the photoresponse over time.

4. SPACE QUALIFICATION

An intensive testing of our 100 packaged detectors pre-selected for flight was performed in particular thermal cycling and response tests. These are illustrated in Fig. 9 showing the spectral response and the photocurrent/voltage curves (under -5 V bias) at room temperature and after all thermal cycling experiments (from 230 to 340 K, and under vacuum or synthetic air) at atmospheric pressure. Performance achieved with the 4 flight-selected detectors are even better since the bias voltage available on the nanosatellite is finally 10 V (response > 100 mA/W).

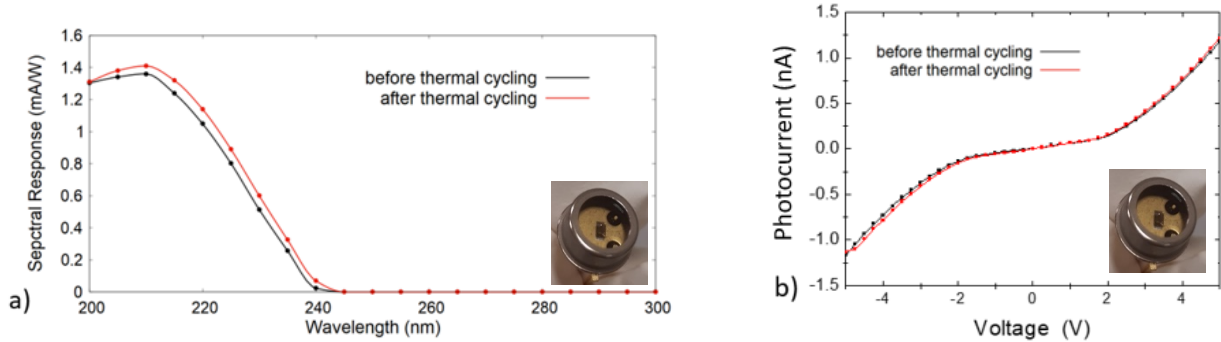


Figure 9. a) Spectral response (at -5 V bias) and (b) IV curves (under polychromatic illumination) at room temperature before (black) and after (red) atmospheric pressure and vacuum thermal cycling of one typical (but with low response) DEVINS UVC β -(Al)Ga₂O₃ detector.

Two versions of our detectors were prepared for the integration in the nanosatellite achieved in October 2022 (cf. Figs. 10 and 11): a long version (DEVINS-L), with a lens focusing the Sun light on the small (500x800 μ m) detector surface to optimize flux collection and increase signal to noise ratio, and a classical one, only with the TO-39 case (with sapphire window) exposed to the Sun (more compact for nanosatellite's accommodation).



Figure 10. Illustrative view of the DEVINS detectors positions on the nanosatellite INSPIRE-SAT 7 and photo of DEVINS-L integration in the nanosatellite (Credits: INSPIRE-SAT 7).

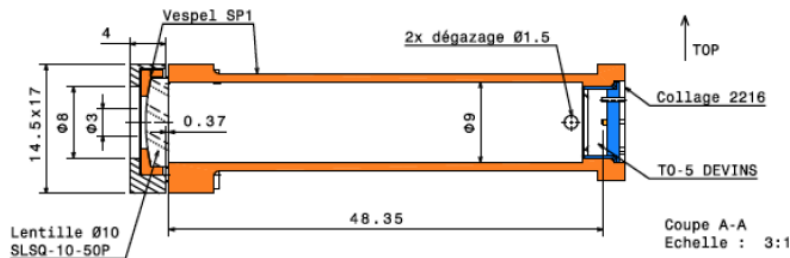


Figure 11. DEVINS-L β -(Al) Ga_2O_3 detector mounting design (with focusing lens) for the INSPIRE-Sat 7 nanosatellite.

Characteristics of our packaged β -(Al) Ga_2O_3 detectors are summarized in Table 1.

Table 1. DEVINS UVC photodetectors characteristics.

PARAMETER	ACHIEVEMENT
Peak response	215/220 nm \pm 5 nm
Spectral response @ peak	> 100 mA/W @ 10 V bias
Spectral range	200–242 nm
Rejection ratio (peak/250 nm)	> 1 000
Mean noise level	< 5 pA
Rise and Fall times	\leq 5 ms

5. CONCLUSION

UVC optimized detectors in Gallium oxide were realized and tested, and present unique performances of extreme solar blindness (factor 1000 or more between peak of responsivity and 250 nm) and dynamical properties (rise and fall times of less than 5 ms). 4 of them are now integrated in the INSPIRE-SAT 7 nanosatellite [5] to be launched in April 2023. Upon success, the DEVINS β -(Al) Ga_2O_3 photodetectors qualified for flight (TRL 8) will be granted TRL 9 (demonstrated in flight).

ACKNOWLEDGEMENTS

These Gallium oxide detectors were realized in the framework of the DEVINS program (DEep uV INnovative detector technologies for Space observations) financed by the ANR (Agence Nationale de la Recherche) under contract ANR-18-CE42-0015 (2018-2022).

REFERENCES

- [1] Rogers, D.J., et al., "Sharp/tuneable UVC selectivity and extreme solar blindness in nominally grown undoped Ga₂O₃ MSM photodetectors by pulsed laser deposition", *Proc. SPIE 11687, 2D-1* (2021).
- [2] Meftah, M., Damé, L., et al., "SOLAR-ISS, a New Solar Spectrum Based on Recent Observations", *Astronomy & Astrophysics* 611 (2018).
- [3] Arrateig, X., Rogers, D.J., Maso, P., et al., "Development and Simulated Environment Testing of β -(Al)Ga₂O₃-based Photodetectors for Space-based Observation of the Herzberg Continuum", *Proc. SPIE 11858, 13* (2021).
- [4] Damé, L., Maso, P., Conan, L., et al., "Realization, calibrations and spatialization of β -(Al)Ga₂O₃ UVC Photodetectors of Extreme Solar Blindness for Space Observations", *Proc. of the 8th International Conference on Sensors and Electronic Instrumentation Advances (SEIA' 2022)*, Ed. Sergey Y. Yurish, IFSA Publishing (2022).
- [5] Meftah, M., et al., "INSPIRE-SAT 7, a Second CubeSat to Measure the Earth's Energy Budget and to Probe the Ionosphere", *Remote Sensing* 14, 186 (2022).